Contents lists available at ScienceDirect

Plant Science

journal homepage: www.elsevier.com

Phosphoglycerate dehydrogenase genes differentially affect Arabidopsis metabolism and development

Rubén Casatejada-Anchel [a, b, 1], Jesús Muñoz-Bertomeu [a, 1], Sara Rosa-Téllez [a, b], Armand D. Anoman [a, b], Sergio G. Nebauer [c], Alejandro Torres-Moncho [a, b], Alisdair R. Fernie [d], Roc Ros [a, b, *]

[a] Departament de Biologia Vegetal, Facultat de Farmàcia, Universitat de València, 46100, Burjassot, Spain
[b] Institut de Biotecnologia i Biomedicina (BIOTECMED), Universitat de València, 46100, Burjassot, Spain
[c] Departamento de Producción vegetal, Universitat Politècnica de València, 46022, Valencia, Spain
[d] Max Planck Institut für Molekulare Pflanzenphysiologie, 14476, Potsdam-Golm, Germany

ARTICLE INFO

Keywords:
PGDH
Phosphoglycerate dehydrogenase
Phosphorylated pathway of serine biosynthesis
PSP
Phosphoserine phosphatase
Serine

ABSTRACT

Unlike animals, plants possess diverse L-serine (Ser) biosynthetic pathways. One of them, the Phosphorylated Pathway of Serine Biosynthesis (PPSB) has been recently described as essential for embryo, pollen and root development, and required for ammonium and sulfur assimilation. The first and rate limiting step of PPSB is the reaction catalyzed by the enzyme phosphoglycerate dehydrogenase (PGDH). In Arabidopsis, the *PGDH* family consists of three genes, *PGDH1*, *PGDH2* and *PGDH3*. *PGDH1* is characterized as being the essential gene of the family. However, the biological significance of *PGDH2* and *PGDH3* remains unknown. In this manuscript, we have functionally characterized *PGDH2* and *PGDH3*. Phenotypic, metabolomic and gene expression analysis in *PGDH* single, double and triple mutants indicate that both *PGDH2* and *PGDH3* are functional, affecting plant metabolism and development. *PGDH2* has a stronger effect on plant growth than *PGDH3,* having a partial redundant role with *PGDH1*. *PGDH3*, however, could have additional functions in photosynthetic cells unrelated to Ser biosynthesis.

1. Introduction

The amino acid L-serine (Ser) is a constituent of proteins, contributing to catalytic functions of many enzymes. Ser is additionally the precursor of other amino acids, is required for the biosynthesis of molecules such as sphingolipids, nitrogen bases or phospholipids, and participates in the metabolism of one-carbon molecules [1].

In plants, there are three metabolic pathways for Ser biosynthesis. One of them, named the glycolate pathway is associated with photorespiration and is exclusive of photosynthetic organisms (Fig. 1). This pathway occurs in the mitochondria, in which two molecules of glycine are converted in one molecule of Ser, in a reaction catalysed by two enzymes, glycine decarboxylase complex and Ser hydroxymethyltransferase releasing NADH, ammonium and CO_2 as side products [2]. The other two nonphotorespiratory pathways are the glycerate pathway and Phosphorylated Pathway of Serine Biosynthesis (PPSB), (Fig. 1). The glycerate pathway occurs in cytosol and peroxisome, while all the PPSB enzymatic reactions take place in plastids [3].

At a quantitative level, the glycolate pathway is the most important, and it is considered to be more active in photosynthetic tissues during daylight hours [4,5]. It has been proposed that the other two pathways could be involved in Ser synthesis mostly in non-photosynthetic tissues. The glycerate pathway has not been studied in detail and its functional significance is unknown mostly due to the lack of a clear genetic evidence for the first committed enzyme of the pathway, the 3-phosphoglycerate phosphatase [6]. However, recent studies have shown that the PPSB is involved in ammonium and sulfur assimilation [7,8] and that it is essential for pollen and embryo development, and crucial for primary root growth in Arabidopsis [7,9–13]. These results would indicate that Ser formed through the PPSB could be necessary for certain cell types and tissues such as meristems where cell division is intense

Abbreviations: AP, aerial parts; PGDH, phosphoglycerate dehydrogenase; PPSB, phosphorylated pathway of serine biosynthesis; PSAT, 3-phosphoserine aminotransferase; PSP, phosphoserine phosphatase; WT, wild type.

* Corresponding author at: Departament de Biologia Vegetal, Facultat de Farmàcia, Universitat de València, Av. Vicent Andrés Estellés S/N, 46100, Burjassot, Valencia, Spain.
Email addresses: Ruben.Casatejada@uv.es (R. Casatejada-Anchel); Jesus.Munoz-Bertomeu@uv.es (J. Muñoz-Bertomeu); Sara.Rosa@uv.es (S. Rosa-Téllez); Armand.Anoman@uv.es (A.D. Anoman); sergonne@bvg.upv.es (S.G. Nebauer); tomona@alumni.uv.es (A. Torres-Moncho); Fernie@mpimp-golm.mpg.de (A.R. Fernie); roc.ros@uv.es (R. Ros)
[1] These authors contributed equally to this work.

https://doi.org/10.1016/j.plantsci.2021.110863
Received 16 November 2020; Received in revised form 25 February 2021; Accepted 25 February 2021
Available online xxx

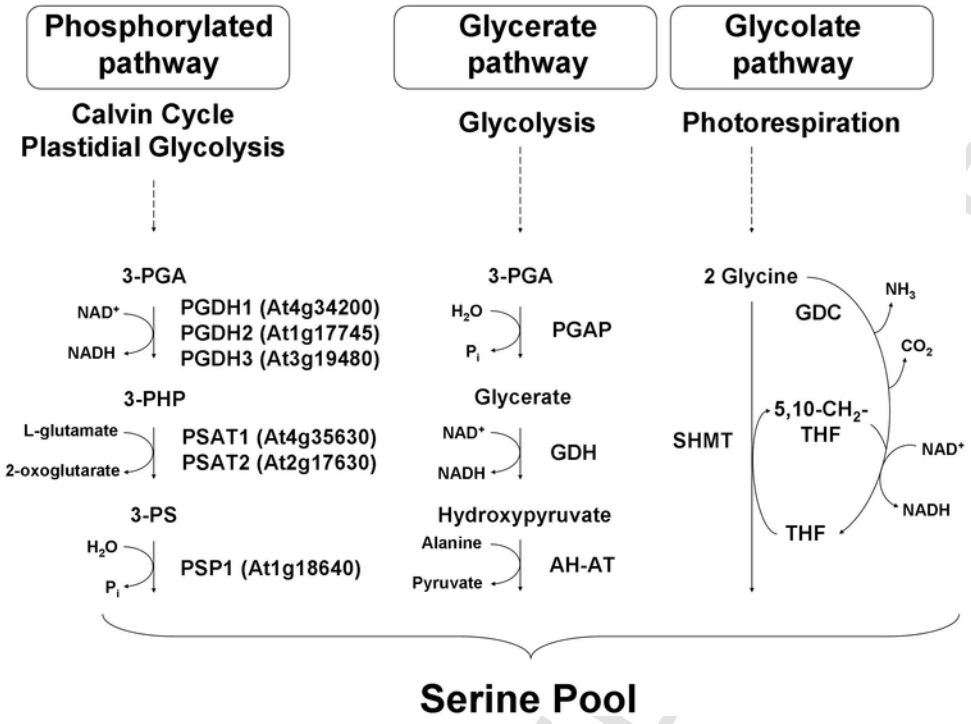

Fig. 1. Schematic representation of the main pathways of Ser biosynthesis in plants. The enzymes participating in each Ser biosynthetic pathway are as follows: glycolate pathway: GDC, glycine decarboxylase; SHMT, Ser hydroxymethyltransferase. Glycerate pathway: PGAP, 3-phosphoglycerate phosphatase; GDH, glycerate dehydrogenase; AH-AT, alanine-hydroxypyruvate aminotransferase. Phosphorylated pathway: PGDH, 3-phosphoglycerate dehydrogenase; PSAT, 3-phosphoSer aminotransferase; PSP, 3-phosphoSer phosphatase. Abbreviations used for metabolites: THF, tetrahydrofolate. 5,10-CH_2-THF, 5,10-methylene-tetrahydrofolate. 3-PGA, 3-phosphoglycerate. 3-PHP, 3-phosphohydroxypyruvate. 3-PS, 3-phosphoSer. This Figure is adapted from Toujani et al. [12].

but where the photorespiration plays a minor contribution to the Ser supply [1,7]. This could be related to the role of Ser as donor of one-carbon units in metabolic processes such as synthesis of nucleic acids.

The PPSB synthesizes Ser from 3-phosphoglycerate in three sequential enzymatic reactions (Fig. 1). The first enzymatic reaction is catalysed by 3-phosphoglycerate dehydrogenase (PGDH) where 3-phosphoglycerate is oxidized utilizing NAD^+ as cofactor to form 3-phosphohydroxypyruvate and NADH (Fig. 1). In the second reaction, catalysed by 3-phosphoSer aminotransferase (PSAT), 3-phosphohydroxypyruvate is transaminated using L-glutamate as the amino donor and releasing 2-oxoglutarate and 3-phosphoSer. In the last step, 3-phosphoSer is converted into Ser in a reaction catalysed by 3-phosphoSer phosphatase (PSP). Three genes for the PGDH have been described, *PGDH1* (At4g34200), *PGDH2* (At1g17745) and *PGDH3* (At3g19480) [10,11], two genes for PSAT, *PSAT1* (At4g35630) and *PSAT2* (At2g17630), [13] and only one for PSP, *PSP1* (At1g18640), [1,9].

Although PSP is encoded by a single gene and PGDH is encoded by three genes, both *PSP1* and *PGDH1* knock-out single mutants display embryo lethal and male gametophyte development defects [7,9,11] confirming that they are essential genes in the pathway. *PGDH1* and *PGDH3* have 78 % amino acid identity between them and show 74 % and 77 % amino acid identity, respectively, with *PGDH2* [11]. The PGDH activity of PGDH2 and PGDH3 has previously been demonstrated [7]. However, *PGDH2* and *PGDH3* knock-out mutants are viable and fertile, without an obvious growth phenotype [11]. Thus, the biological significance of *PGDH2* and *PGDH3* remains unknown. In this work we have studied the role of these two genes in plant development and Ser metabolism through phenotypic and molecular characterization of a combination of single, double and triple mutants of the PGDH gene family. We concluded that *PGDH1* and *PGDH2* co-operate in Ser metabolism and are functionally closer than *PGDH3*, while this latter could have additional functions in photosynthetic cells unrelated to Ser biosynthesis.

2. Materials and methods

2.1. Identification and isolation of mutants, cloning and plant transformation

Original Arabidopsis (*Arabidopsis thaliana*) seed stocks (ecotype Columbia-0) were supplied by the European Arabidopsis Stock Center [14]. Conditional mutants of *PSP1* (*c-psp1-1*), single mutants of *PGDH1* (*pgdh1-2*), *PGDH2* (*pgdh2-2, pgdh2-3*) and *PGDH3* (*pgdh3-1, pgdh3-2*) were obtained or isolated previously [9,11] and renamed by Ros et al. [1]. Conditional *c-pgdh1-2 lines* were obtained by transforming *pgdh1-2* homozygous mutant [1,11] with a construct carrying the *PGDH1-GFP* cDNA under the control of the heat shock inducible promoter of gene *HSP18.2* (At5g59720). The *35S* promotor of a previous construct carrying *PGDH1-GFP* (*Pro35S:EDA9*; [11]) in plasmid pMDC83 [15] was exchanged with a 852-bp fragment corresponding to the promoter region of *HSP18.2* between the *Pme*I and *Spe*I sites to give the construct *ProHSP18.2:PGDH1*. The *35S* promotor of construct *Pro35S:EDA9* was also exchanged with a 1514-bp fragment corresponding to the native *PGDH1* promoter to give the construct *ProPGDH1:PGDH1* as previously described [11]. As *pgdh1-2* is embryo-lethal, the heterozygous *PGDH1 pgdh1.2* plants were transformed with this construct using the floral dipping method [16] with *Agrobacterium tumefaciens* carrying pSOUP. Transformants were selected by antibiotic selection, while homozygous *pgdh1-2 pgdh1-2* were identified by PCR genotyping using gene-specific primers (PD LP6 and PD RL6) and left border primers of the T-DNA insertions (Gabi 8409), (Supplementary Table S1). Five independent single insertion homozygous T3 lines were obtained.

Double and triple mutants were obtained by crosses of single mutants *pgdh2-3*, *pgdh3-1* and the conditional mutant *c-pgdh1-2*, giving the double mutants *c-pgdh1-2 pgdh2-3*, *c-pgdh1-2 pgdh3-1*, *pgdh2-3 pgdh3-1* and the triple mutant *c-pgdh1-2 pgdh2-3 pgdh3-1*. Homozygous double

and triple mutants were selected with antibiotics and verified by PCR genotyping using gene-specific primers and left border primers of the T-DNA insertion (Supplementary Table S1).

2.2. Growth conditions

Seeds were sterilized and sown on 0.8 % agar plates containing one-fifth-strength Murashige and Skoog medium (1/5 MS) with Gamborg vitamins buffered with 0.9 g L^{-1} MES, adjusted to pH 5.7 with Tris. After 2–4 days of stratification at 4 °C, plates were vertically placed at 22 °C for 14–16 days with a 16-h-day/8-h-night photoperiod at 100 μmol m^{-2} s^{-1}. In experiments where double and triple mutants were compared, plates were supplemented with 0.5 % sucrose.

Some seeds were also grown under greenhouse conditions in pots filled with a (1:1, v/v) mixture of vermiculite and fertilized peat (Kekkilä 50/50; kekkilä Iberia, S.L.) irrigated with demineralized water as required. Trays were placed in a cold chamber (4 °C) and were placed under the greenhouse staging after 4 days. Growth conditions consisted of 16 h light, 50–70 % relative humidity and an average temperature of 24 °C during the daytime and 17 °C during the night. Whenever necessary, these conditions were supplied with artificial light from sodium and mercury vapor lamps.

2.3. Gene expression analysis and western blot

For the gene expression analysis, 15–40 day-old plants vertically grown in plates or in pots under greenhouse conditions were used. Plants were sampled after 8–9 h in the light. Total RNA was extracted using the NucleoSpin RNA II kit (Macherey-Nagel). RNA (0.5–1 μg) was reverse transcribed using polyT primers and the first-strand cDNA synthesis kit for quantitative RT-PCR (Thermo Fisher Scientific) according to the manufacturer's instructions. Real-time quantitative PCR was performed using a 5700 sequence detector system (Applied Biosystems) with the Power SYBR Green PCR Master Mix (Applied Biosystems) according to the manufacturer's protocol. Each reaction was performed in triplicate with 1 μL first-strand cDNA in a total volume of 20 μL. Data are the mean of three biological samples. PCR amplification specificity was confirmed with a heat dissociation curve (from 60 to 95 °C). Reference genes were selected [17]. Relative mRNA abundance was calculated using the comparative cycle threshold method according to Pfaffl [18]. When required, the obtained values were corrected by the efficiency of PCR amplification for each pair of primers. Primers used for PCRs are listed in Supplementary Table S1. For *PGDH1* induction, plants were sampled 1 h after a heat-shock treatment (1 h at 37 °C).

For western blots, crude protein extracts were obtained by harvesting 0.5 g of plant material in liquid nitrogen and grinding in 1 mL of ice-cold homogenization buffer (140 mM NaCl, 8 mM $Na_2HPO_4.7H_2O$, 2 mM KH_2PO_4, 10 mM KCl, pH 7.4) with 1% of the Protease Inhibitor Cocktail (Sigma, P-9599), followed by two successive centrifugations (15,000 *g* for 15 min at 4 °C). Protein samples were quantified with Bradford reagent (Bio-Rad) using bovine serum albumin as a standard, and then 100 μg of total proteins were separated in 8% SDS-PAGE. Proteins were electrotransferred onto Immune-Blot nitrocellulose membranes (Bio-Rad) using the Mini Tran-Blot Cell (Bio-Rad) for 1 h at 100 V with the transfer buffer [17 mM Tris, 192 mM glycine, and 20 % (v/v) methanol]. Immunoblots were probed with anti-GFP antibodies (Molecular probes, ref. A-11122) at final dilution of 1:10,000. Cross-reacting bands were detected using the ECL select Western-Blotting detection reagent kit (Amersham Biosciences). For PGDH1 induction, plants were sampled 8 h after a heat-shock treatment (1 h at 37 °C).

2.4. Metabolite determination

AP and roots of 15-day-old plants grown on vertical plates were used to determine metabolite content in derivatized methanol extracts by gas chromatography-mass spectrometry using the protocol defined by Lisec et al. [19]. Plants were sampled after 8–9 h in the light.

2.5. Photosynthetic activity measurements

Simultaneous gas exchange measurements were taken with a LICOR-6400 (LICOR Biosciences, NE, USA) as described by Faus et al. [20]. Net CO_2 fixation rate (AN), stomatal conductance (gs) and substomatal CO_2 concentration (Ci) were measured at steady state under conditions of saturating light (1000 μmol m^{-2} s^{-1}) and 400 ppm CO_2. Simultaneous chlorophyll *a* fluorescence determinations were performed. The actual effective quantum efficiency of photosystem II (PhiPS2) was determined by measuring steady-state fluorescence (Fs) and maximum fluorescence (Fm') during a light-saturating pulse (8000 μmol m^{-2} s^{-1}) with the LICOR-6400. Photorespiration rates were estimated from combined gas exchange and chlorophyll fluorescence determinations according to Valentini et al. [21]. Plants were grown in pots under greenhouse conditions for 30 days. Measurements were taken 2 h after the beginning of the light period to allow full photosynthesis activation.

2.6. Statistical analysis and bioinformatics

Experimental values represent mean values and standard error; n represents the number of independent samples. Significant differences as compared to WT were analyzed by Student's t-tests algorithms (two-tailed) using Microsoft Excel. Statistical differences between groups were analyzed with a one-way ANOVA and further post hoc test (Tukey's b or Games-Howell) with the IBM SPSS Statistics software. The level of significance was fixed at 5% (0.05).

Phylogenetic and molecular evolutionary analyses were conducted using MEGA version X [22]. The analysis based on gene expression was done using the expressolog tree viewer at the bioanalytical resource for plant biology [23]. The 2-gene plot expression and co-expression analysis was done with curated transcriptomic data from public repositories using the Genevestigator tool [24]. The PPSB interactions were obtained using the GeneMANIA tool [25].

3. Results

3.1. PGDH2 and PGDH3 are functional genes

Quantitative expression analyses of *PGDH* genes indicated that *PGDH1* is the major gene of the family in all organs studied at both seedling and mature stages, followed by *PGDH2* (Fig. 2A, B). Both *PGDH1* and *PGDH2* are mostly expressed in roots of seedlings and adult plants, but they are also expressed in siliques, flowers, shoot and leaves. However, *PGDH3* is expressed almost exclusively in aboveground tissues, mainly in leaves, being almost undetectable in roots, which confirm previous gene expression studies [7,11]. According to the Genevestigator tool (https://genevestigator.com/) *PGDH1* is highly expressed at early stages of development (germination and seedling stages), but its expression is maintained high at all stages of the plant cycle. *PGHD2* has an opposite trend, progressively increasing expression from seedling stage till late developmental stages (developed flower and mature silique developmental stages). *PGDH3* expression, however, is higher at mature stages coinciding with the full photosynthetic capacity of the plant and is less expressed at early and late stages of plant development.

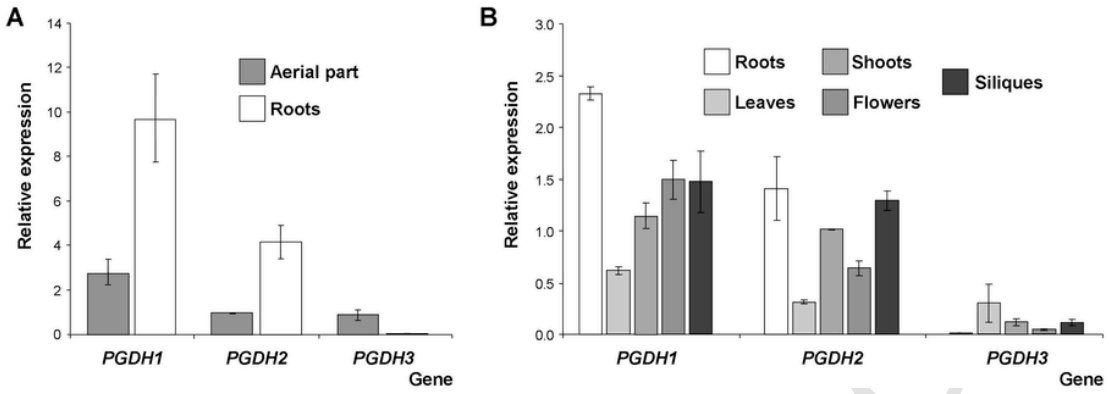

Fig. 2. Quantification of *PGDH* gene family expression. (A) qRT-PCR analysis of *PGDH* genes in the aerial part (AP) and roots of 15-day-old seedlings grown in plates. (B) expression analysis in different adult (40-day-old) plant organs grown under greenhouse conditions. Values (mean ± SE; n = 3 independent biological replicates) are normalized to the expression of *PGDH2* in the AP (A), or shoots (B).

Characterization of Arabidopsis lines silenced in the *PGDH1* gene, showed that plants have a strong reduction in the primary root growth [7], a phenotype also observed in conditional mutants of *PSP1* (*c-psp1-1*), the single gene coding for the last enzyme of PPSB [9]. *c-psp1-1* is a line in which a cDNA of *PSP1* is expressed in a knock-out *psp1* mutant under the control of a heat-shock inducible promoter [9]. This mutant has low background levels of *PSP1* expression under non-inductive conditions which makes it viable and thus suitable for studying the *PSP1* function during plant vegetative development [8,9]. We made conditional *PGDH1* mutants (*c-pgdh1-2*) by expressing the *PGDH1* cDNA in a knock-out *PGDH1* mutant (*pgdh1-2*) under the control of the same heat-shock inducible promoter used *for c-psp1-1*. Five *c-pgdh1-2* lines were obtained with different levels of *PGDH1* expression (Fig. 3A). When grown in plates under non inductive conditions, the five *c-pgdh1-2* lines displayed reduced primary root growth, the most characteristic phenotype of all PPSB-deficient lines [7,9] (Fig. 3B). However, this parameter was much strongly reduced in *c-psp1-1* than in *c-pgdh1-2* lines (Fig. 3B). Two of the *c-pgdh1-2* lines (*c1-pgdh1-2*, *c2-pgdh1-2*), exhibiting the strongest primary root growth reduction and lowest *PGDH1* expression, were selected for further analysis. *c1-pgdh1-2*, *c2-pgdh1-2* showed lower basal PGDH1 protein levels than controls expressing *PGDH1* under the control of the native promoter (Fig. 3C). These lines recovered root growth by both Ser supplementation or *PGDH1* induction (Fig. 3D, E). In adult stage *c1-pgdh1-2* and *c2-pgdh1-2* were sterile, another phenotype associated to PPSB deficiency (Supplementary Fig. S1). The fertility was rescued by inducing *PGDH1* in these lines (Supplementary Fig. S1).

In order to further study the effect of *PSP1* and *PGDH1* in the plant vegetative development, the two *c-pgdh1-2* (*c1-pgdh1-2*, *c2-pgdh1-2*) and *c-psp1-1* (*c1-psp1-1* and *c2-psp1-1*) lines with the strongest phenotypes were compared (Fig. 4). In addition to the reduced primary root growth, the c-*pgdh1-2* lines also showed reduced root fresh weight, while *c-psp1-1* lines were affected in both roots and aerial parts (AP) fresh weight as compared to wild type controls (WT) (Fig. 4B, C). Growth of PPSB conditional mutant lines in pots under greenhouse conditions, showed that the rosette fresh weight was also more diminished in *c-psp1-1* than in *c-pgdh1-2* lines as compared to WT, thus confirming that *c-psp1-1* showed more drastic phenotypes than c-*pgdh1-2* (Fig. 4D). Consequently, these results suggested that *PGDH2* and *PGDH3* in the *c-pgdh1-2* background could contribute to plant growth.

Single homozygous *PGDH2* mutant alleles (*pgdh2-2*, *pgdh2-3*) did not display obvious growth phenotypes when cultivated in plates while both *PGDH3* mutant alleles (*pgdh3-1*, *pgdh3-2*) showed about 15–25 % reduced AP growth (Fig. 5, A–E). Interestingly, combinations of *PGDH2* and *PGDH3* double mutants (*pgdh2-2 pgdh3-2*, *pgdh2-3 pgdh3-1*) did not produce stronger growth phenotypes than single mutants (Fig. 5). In fact, the stronger the phenotype of the *PGDH3* mutant allele, the weaker the phenotype of the double mutant. Thus, only one of the double mutant combination (*pgdh2-3 pgdh3-1*) displayed a lower AP fresh weight compared to WT (Fig. 5B). Under greenhouse conditions, there was a general reduction of the rosette fresh weight of PPSB single and double mutants (about 20–30 %) as compared to WT (Fig. 5E). However, no significant differences in growth were found between single and double mutants in any of the measured parameters, neither in plates nor in pots (Fig. 5) suggesting that, in spite of having a different expression pattern, *PGDH2* and *PGDH3* did not have an additive effect on plant growth.

To further confirm these results, we performed a metabolomic study of *PGDH* mutants. We selected the double mutant allele combination showing significant AP growth reduction as compared to the WT, along with the single mutant alleles. According to the Principal Component Analysis (PCA), the metabolite profile of single mutants *pgdh2-3* and *pgdh3-1* was different in both roots and AP and did not overlap with that of the WT (Fig. 6A). In the AP, those metabolites which better explained differences between *pgdh2-3* and *pgdh3-1* according to the PCA were glyceric acid and maltose (Supplementary Fig. S2). Glyceric acid level was reduced by 50 % in *pgdh3-1* compared to the WT. Maltose was the most highly increased metabolite in this mutant (128 %), while it was reduced in *pgdh2-3*. In roots, the most important changes between single mutant lines were attributed to isoleucine, lysine, glutamine and isocitric acid, which displayed opposite trends. It is interesting to remark that glyceric acid levels were again lowest in *pgdh3-1* than in the other backgrounds.

The metabolite profile of the *pgdh2-3 pgdh3-1* double mutant, was also different to that of the single mutants (Fig. 6A). Interestingly, it partly overlapped with that of the WT in both AP and roots. Thus, in the double mutant several metabolites showed an intermediate value as compared to the single mutants as visualized in the heatmap (Fig. 6B; Supplementary Tables S2 and S3). A clear example of this behavior is the metabolite Ser which was reduced in *pgdh2-3* and increased in *pgdh3-1* as compared to WT, while having an intermediate value in *pgdh2-3 pgdh3-1* (Fig. 6C). Other metabolites in the *pgdh2-3 pgdh3-1* AP such as glyceric acid, lysine, arginine and methionine showed levels similar to WT. Besides, metabolites like ornithine, proline and raffinose displayed an opposite trend to that of the single mutants. In roots, isoleucine and isocitric acid approached WT levels while others like glyceric acid and putrescine displayed an opposite trend to that of the single mutants.

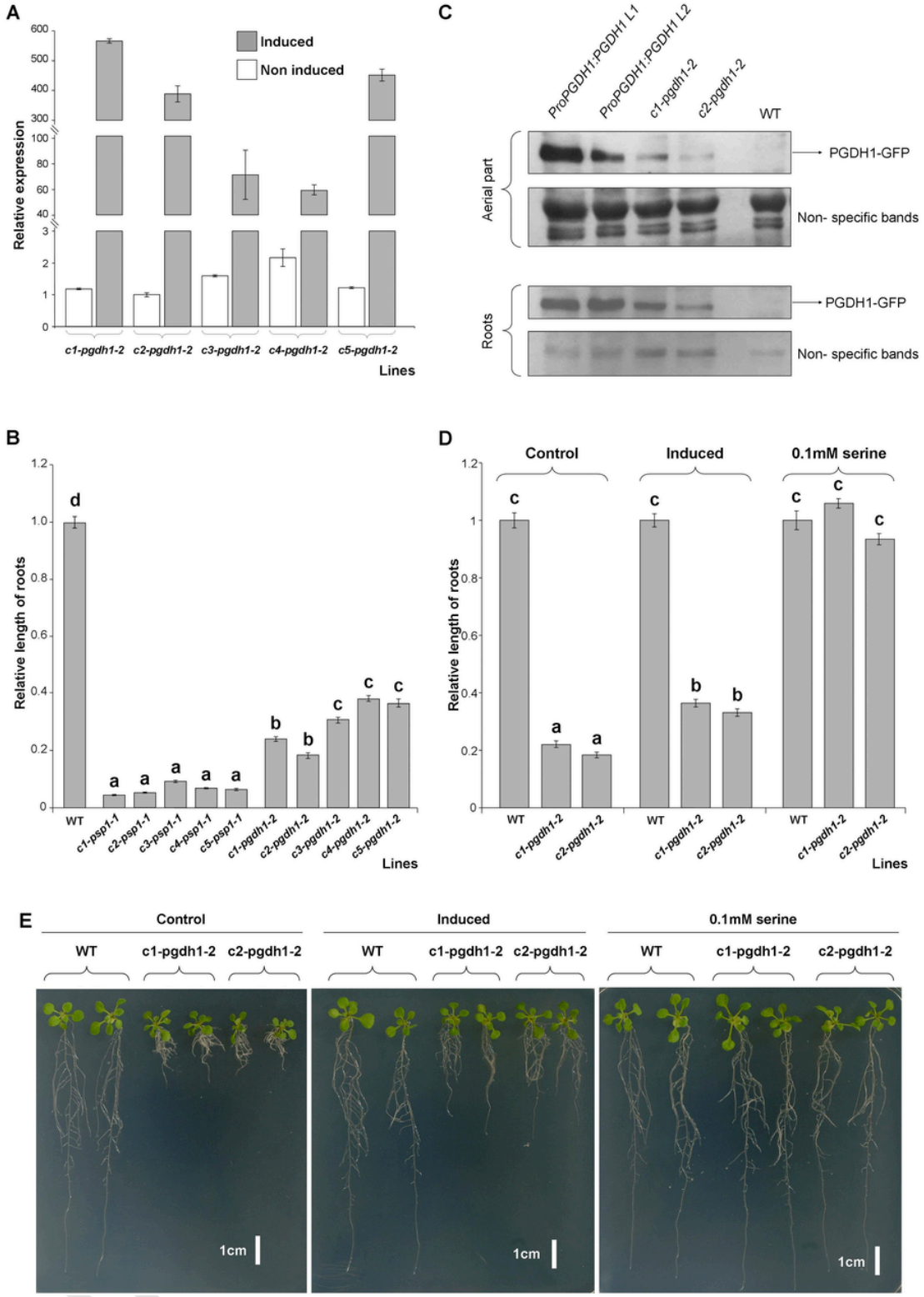

Fig. 3. Phenotypic and molecular characterization of *PGDH1* and *PSP1*conditional mutants (*c-pgdh1-2* and *c-psp1-1*) grown in plates (13-day-old seedlings) or greenhouse conditions (46-day-old mature plants). (A) qRT-PCR analysis of *PGDH1* expression in five single homozygous transgenic lines before and after *PGDH1* induction by a heat-shock treatment. *PGDH1* levels were normalized to the lowest value of *c2-pgdh1-2* line. (B) Primary root length of *c-pgdh1-2* and *c-psp1-1* lines grown in plates. (C) Western blot showing the expression of PGDH1-GFP fusion protein in the aerial part (AP) and roots of wild-type (WT) and *pgdh1* mutants complemented with either the *PGDH-GFP* cDNA under de control of the heat shock promoter (*c1-pgdh1-2, c2-pgdh1-2*) or the native *PGDH1* promoter (*ProPGDH1:PGDH1 L1, ProPGDH1:PGDH1 L2*). Plants were grown under non inductive conditions. The signal of a non-specific band is shown as sample loading control in the bottom panel. (D) Primary root length of *c-pgdh1-2* lines lines under induced conditions or in the presence of 0.1 mM Ser. (E) Picture of representative individuals grown under induced conditions or in the presence of 0.1 mM Ser. Phenotipic data are the mean ± SE; $n \geq 60$ plants) Different letters indicate significant differences between lines ($P < 0.05$).

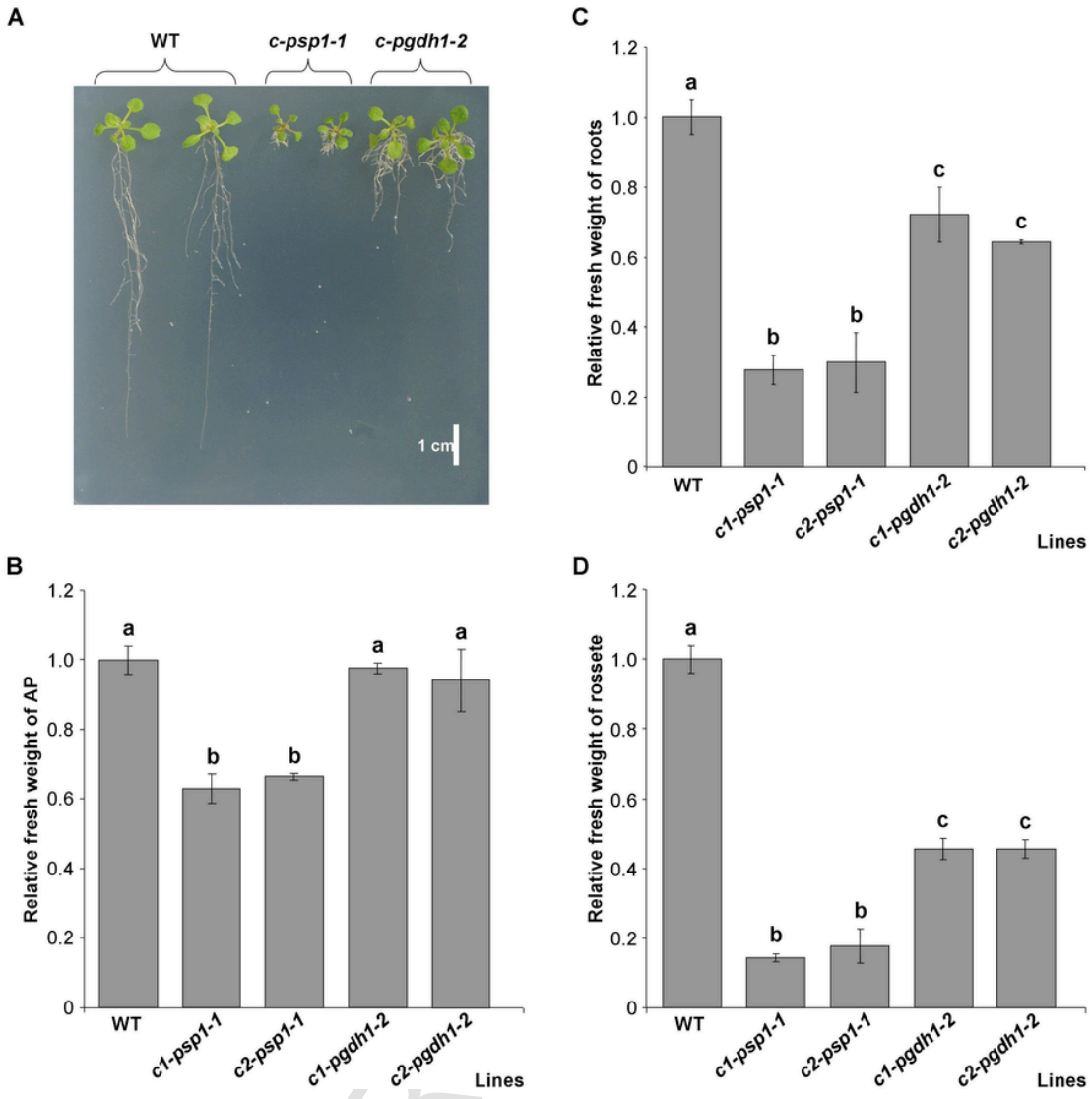

Fig. 4. Comparison of *PGDH1* and *PSP1*conditional mutants (*c-pgdh1-2* and *c-psp1-1*) grown in plates (17-day-old seedlings) or greenhouse conditions (46-day-old mature plants). (A) Picture of a representative individual of each line grown in plates. (B, C) Fresh weight (FW) of aerial parts (AP) and roots of *c-psp1-1* (*c1-psp1-1* and *c2-psp1-2*), *c-pgdh1-2* (*c1-pgdh1-2* and *c2pgdh1-2*) and wild type (WT) seedlings grown in plates. (D) Rosette FW of mature plants grown in pots under greenhouse conditions. Values (mean ± SE; $n \geq 100$ plants) are normalized to the mean calculated for the WT. Different letters indicate significant differences between lines ($P < 0.05$).

3.2. Phenotypic and metabolomic characterization of PGDH double and triple mutants

In order to understand the functional connections between *PGDH* genes we generated additional combinations of *PGDH1/PGDH2/PGDH3* by generating double and triple mutants. Two different lines with similar phenotypes were obtained for each combination (*c1-pgdh1-2 pgdh2-3, c1-pgdh1-2 pgdh3-1*, *c1-pgdh1-2 pgdh2-3 pgdh3-1; c2-pgdh1-2 pgdh2-3, c2-pgdh1-2 pgdh3-1*, *c2-pgdh1-2 pgdh2-3 pgdh3-1*). Data presented are mean values of these two lines, which were generically named as *c-pgdh1-2 pgdh2-3, c-pgdh1-2 pgdh3-1* and *c-pgdh1-2 pgdh2-3 pgdh3-1*. *PGDH* double and triple mutants were phenotypically evaluated in plates (Fig. 7A, C–E) and in greenhouse (Fig. 7B, F). Both *PGDH2* and *PGDH3* had an effect of plant growth in a c-*pgdh1* mutant background. Opposite to what was observed in a WT background, this effect was greater for *PGDH2* than for *PGDH3* in all parameters studied (Fig. 7). In plates, *c-pgdh1-2 pgdh2-3* displayed the strongest growth phenotype resembling that of *c-psp1-1* lines (Figs. 3A, 4A, 7A). Compared to *c-pgdh1-2 pgdh2-3*, the *c-pgdh1-2 pgdh3-1* lines presented much weaker growth reduction when considering AP and root fresh weight (Fig. 7C, D). In relation to these growth parameters, the triple *c-pgdh1-2 pgdh2-3 pgdh3-1* was not smaller than the double *c-pgdh1-2 pgdh2-3* neither in AP nor in roots (Fig. 7A, C, D). Besides, the primary root growth was more strongly affected in the double *c-pgdh1-2 pgdh2-3* mutant than in the triple *c-pgdh1-2 pgdh2-3 pgdh3-1* mutant (Fig. 7A, E), suggesting that *PGDH3* mutation had a positive effect in the primary root growth when *PGDH1* and *PGDH2* were also mutated. This positive effect on growth was confirmed when mutant lines were evaluated in greenhouse conditions, where the triple mutant performed better that the double mutant *c-pgdh1-2 pgdh2-3* (Fig. 7B, F).

The PCA of the metabolite profiles of double and triple *PGDH* mutants indicated that the *c-pgdh1-2 pgdh2-3* and *c-pgdh1-2 pgdh2-3 pgdh3-1* mutants were clearly separated from the other mutants, especially in roots (Fig. 8A). Interestingly, in the AP, the triple c-*pgdh1-2 pgdh2-3 pgdh3-1* mutant was closer to the WT than the double c-*pgdh1-2 pgdh2-3* mutant (Fig. 8A). In roots, however, the PCA of the double c-*pgdh1-2 pgdh2-3* mutant and triple mutants were more similar, agreeing with the low expression levels of *PGDH3* in this organ (Fig. 8A). When the metabolite changes were represented as a heatmap, they revealed that

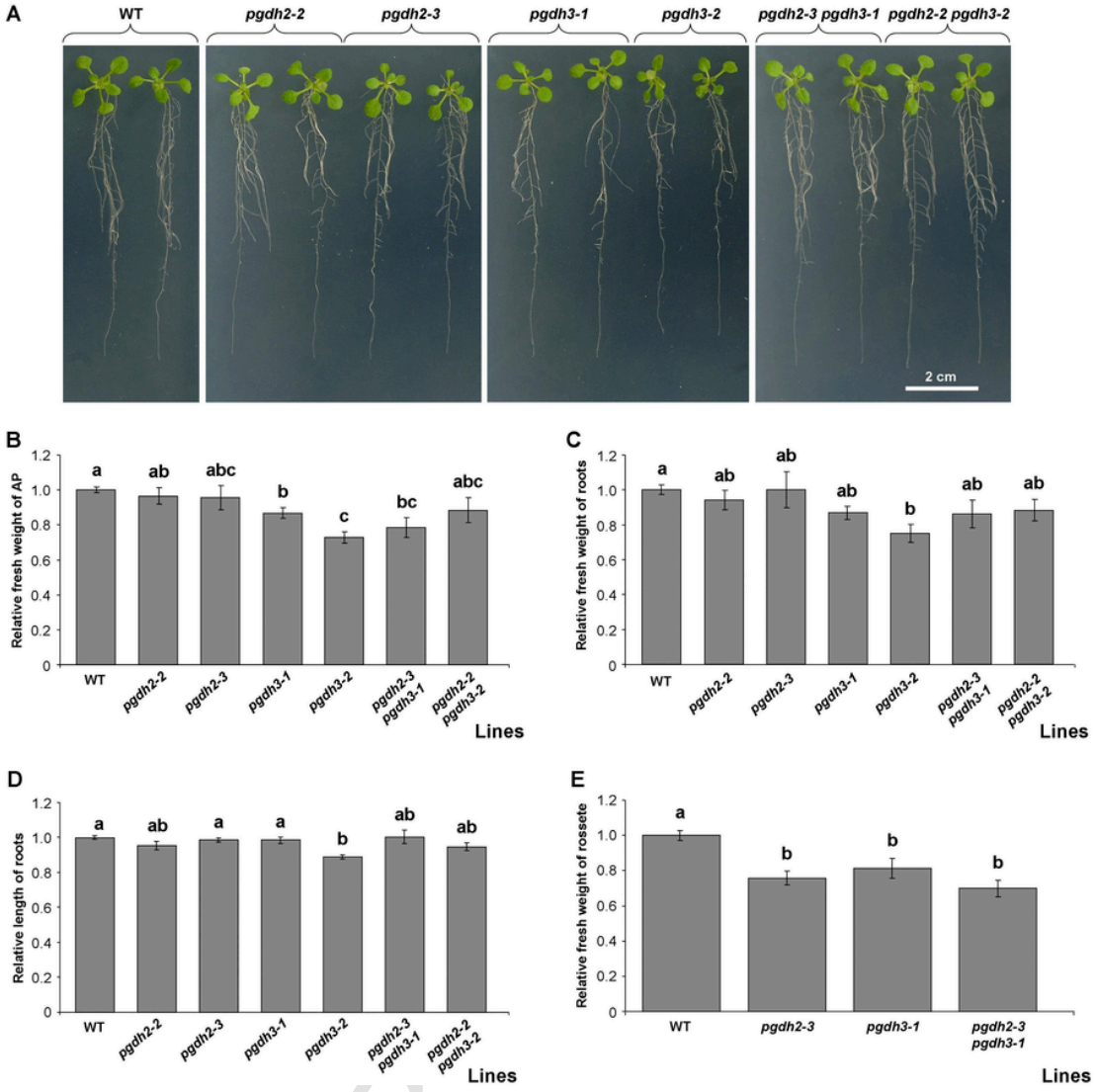

Fig. 5. Phenotype of *PGDH2* and *PGDH3* single and double mutants (*pgdh2-2, pgdh2-3, pgdh3-1, pgdh3-2, pgdh2-3 pgdh3-1 and pgdh2-2 pgdh3-2*) grown in plates (15-day-old seedlings) or greenhouse conditions (46-day-old mature plants). (A) Picture of a representative individual of each line grown in plates. (B, C) Fresh weight (FW) of aerial parts (AP) and roots of single and double mutants, and wild type (WT) seedlings grown in plates. (D) Primary root length of lines grown in plates. (E) Rosette FW of mature plants grown in pots under greenhouse conditions. Values (mean ± SE; $n \geq 100$ plants) are normalized to the mean calculated for the WT. Different letters indicate significant differences between lines ($P < 0.05$).

the *c-pgdh1-2 pgdh2-3* mutant is the line where most drastic changes were observed as compared to the WT, especially in the AP (Fig. 8B and Supplementary Tables S4 and S5). In general, there was an increase of metabolite levels in all the double and triple mutants. Those metabolites which better explained differences between double and triple mutants in the AP according to the PCA were asparagine, glutamine, glycine and trehalose (Supplementary Fig. S3). The asparagine and glutamine levels were the highest in the *c-pgdh1-2 pgdh2-3* mutant. The high levels of some amino acids were attenuated in the triple *c-pgdh1-2 pgdh2-3 pgdh3-1* mutant as compared to the double *c-pgdh1-2 pgdh2-3* mutant, especially those of glutamine (Fig. 8B and Supplementary Tables S4 and S5). The trehalose levels were increased in all the mutants except in the *c-pgdh1-2 pgdh3-1* in which there were reduced. As in *pgdh3-1*, the mutation in *PGDH3* reduced the glyceric acid levels in both double *c-pgdh1-2 pgdh3-1* and triple *c-pgdh1-2 pgdh2-3 pgdh3-1* as compared to the other mutant backgrounds where PGDH3 was functional. In roots, all mutant backgrounds displayed an increased level of amino acids such as alanine, asparagine or glutamine. Unlike the AP, the attenuating effect observed in the triple *c-pgdh1-2 pgdh2-3 pgdh3-1* as compared to the double was not observed. The metabolites which better explained differences between lines were trehalose and serine. The trehalose levels were much more increased in the *c-pgdh1-2 pgdh2-3* and *c-pgdh1-2 pgdh2-3 pgdh3-1* than in the *c-pgdh1-2* and *c-pgdh1-2 pgdh3-1* mutant backgrounds as already observed in the AP. Changes in Ser levels in *PGDH* mutants were particularly interesting (Fig. 8C). In the AP, the Ser levels of all the double and triple mutants (*c-pgdh1-2, c-pgdh1-2 pgdh2-3, c-pgdh1-2 pgdh3-1* and *c-pgdh1-2 pgdh2-3 pgdh3-1*) were higher than in WT, especially in those mutants showing the most drastic phenotypes (*c-pgdh1-2 pgdh2-3* and *c-pgdh1-2 pgdh2-3 pgdh3-1*). In roots, however, the Ser levels were lower than in WT in these lines with more drastic phenotypes, while they were higher than in WT in lines *c-pgdh1-2 and c-pgdh1-2 pgdh3-1* mutants.

3.3. Reduced PGDH1 expression triggers PGDH2 and represses PGDH3 expression

The phylogenetic analysis of *PGDH* gene family based on sequence similarity indicated that *PGDH1* and *PGDH3* are more closely related to one another than to *PGDH2* [11], (Fig. 9). However, the analysis of *PGDH* genes expression pattern under different environmental condi-

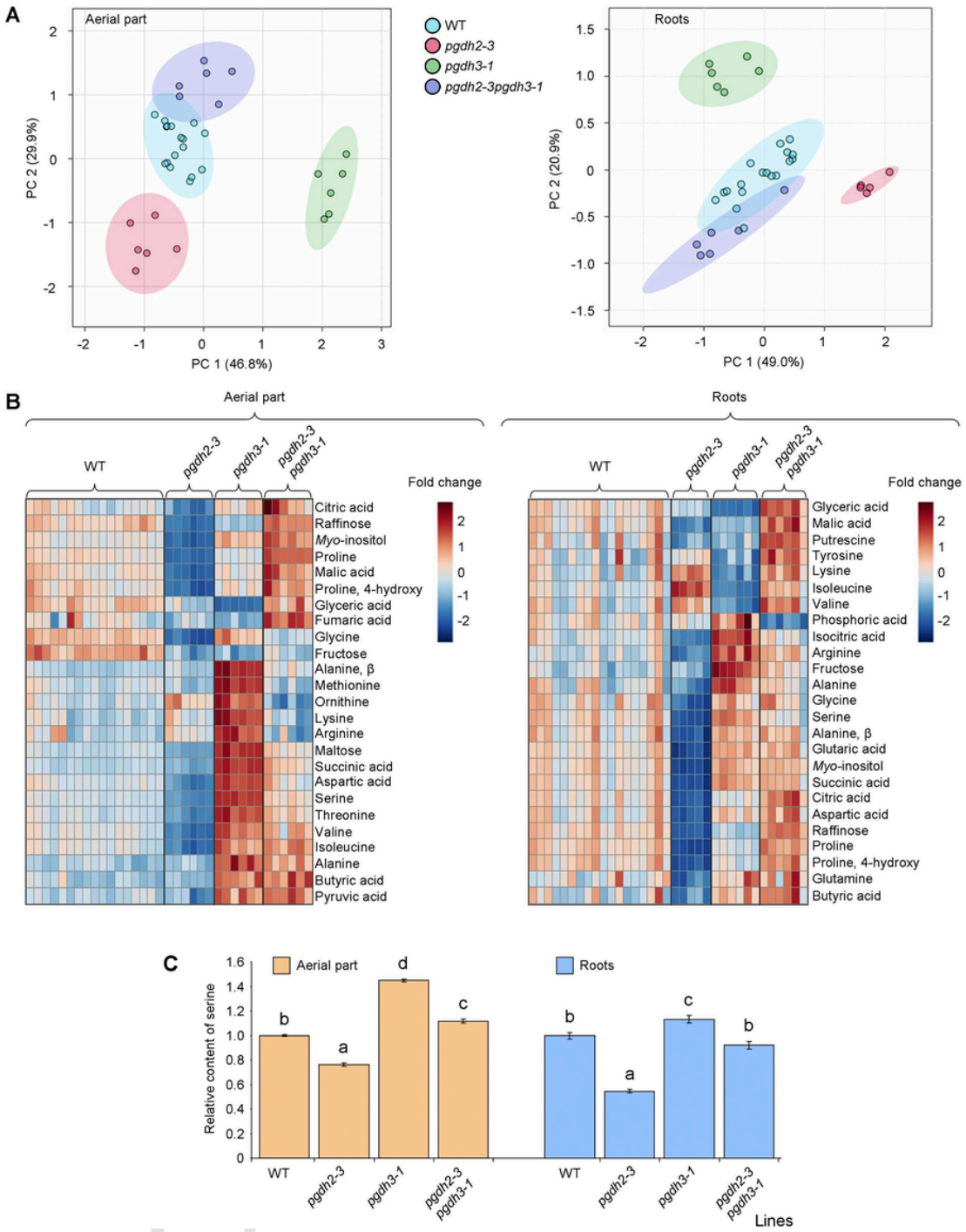

Fig. 6. Metabolite profile of *PGDH2* and *PGDH3* single and double mutants (*pgdh2-3, pgdh3-1, pgdh2-3 pgdh3-1*). (A) Principal component analysis (PCA) of the metabolite profiles of *PGDH* mutant lines in aerial parts (AP) and roots. Data from the GC–MS analysis were evaluated using the PCA with the two first components accounting for at least 70 % of total metabolic variance. Values in parenthesis give the relative contribution of each component to the total variance observed in the dataset. (B) Most relevant changes in the metabolite content of AP and roots of *PGDH* mutants as compared with the wild type (WT). Values of the relative metabolic contents are presented as a heat map. (C) Relative Ser content in different lines. Values represent the mean ± SE, $n \geq 6$ pools of 40 plants. Different letters indicate significant differences between lines ($P < 0.05$). Detailed results of the assay are presented in Supplementary Tables S2 and S3.

tions (http://bar.utoronto.ca/), indicated that *PGDH1* and *PGDH2* were more closely related than *PGDH3* (Fig. 9). Accordingly, a 2-gene plot expression analysis of *PGDH* genes using *mRNAseq* data (https://genevestigator.com/) showed a positive correlation between *PGDH1* and *PGDH2* gene expression under different environmental conditions. *PGDH3*, however, showed a negative correlation with the other two *PGDH* genes (Supplementary Fig. S4).

In order to understand the functional connections between *PGDH* genes, we performed a gene expression analysis in *PGDH* single, double and triple mutants. Neither *PGDH2* nor *PGDH3* were induced in the single *pgdh3-1* and *pgdh2-3*, respectively. *PGDH1* expression was also unchanged in single *pgdh2-3, pgdh3-1*, and in the double *pgdh2-3 pgdh3-1* (Fig. 10A and B). However, the absence of *PGDH1* induced *PGDH2* in the AP (Fig. 10C). This inductive effect could be seen in both single

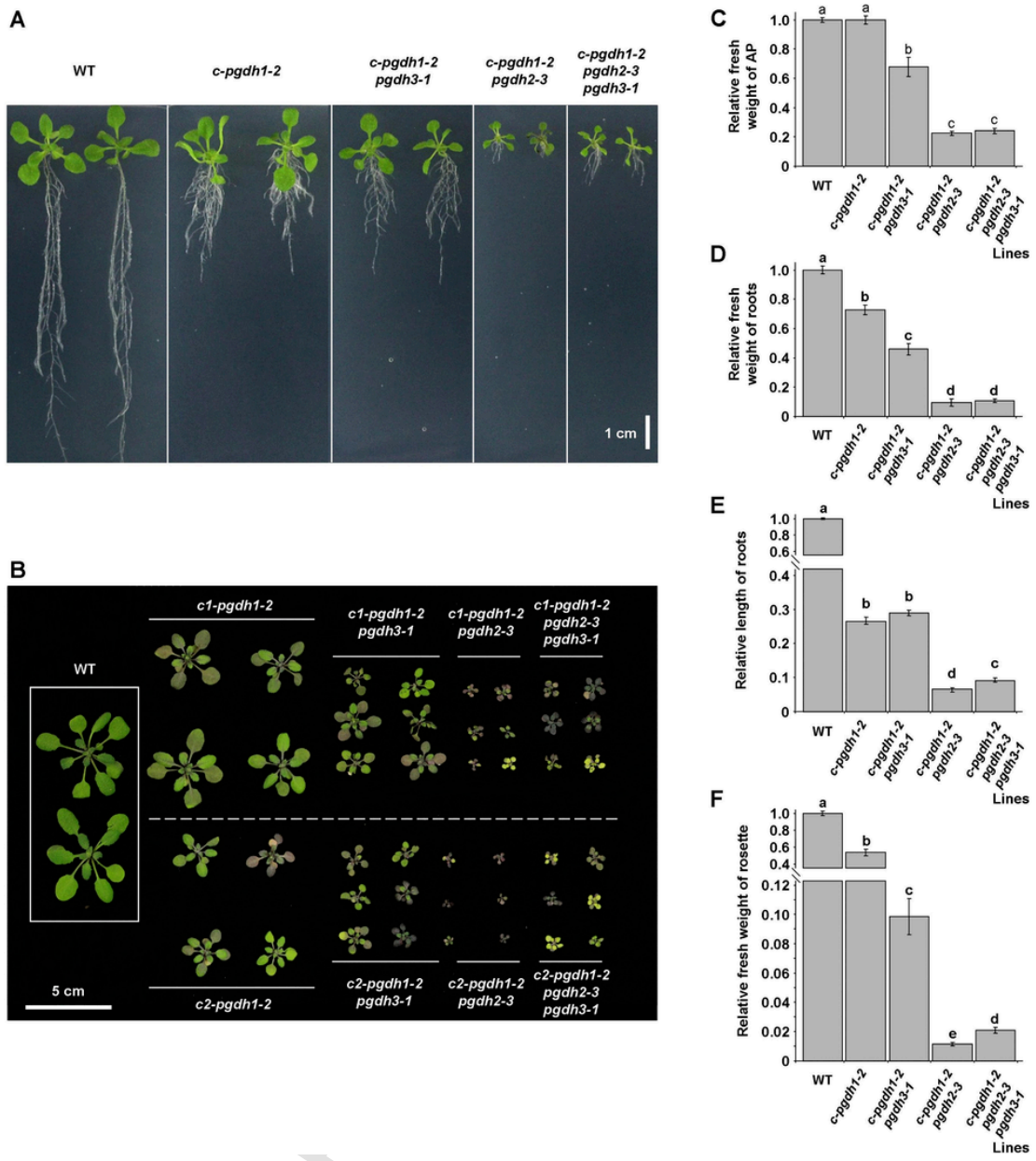

Fig. 7. Phenotype of *PGDH* family double and triple mutants (*c-pgdh1-2 pgdh2-3, c-pgdh1-2 pgdh3-1*, *c-pgdh1-2 pgdh2-3 pgdh3-1*) grown in plates (14-day-old seedlings) or greenhouse conditions (24-day-old mature plants). (A) Picture of a 15-day-old representative individuals of each line grown in plates. (B) Picture of a 24-day-old representative individuals of each line grown in greenhouse conditions. (C, D) Fresh weight (FW) of aerial parts (AP) and root seedlings of different lines grown in plates as compared to wild type (WT). (E) Primary root length of lines grown in plates. (F) Rosette FW of mature plants grown in pots under greenhouse conditions. Values (mean ± SE; $n \geq 100$ plants from two different lines for each genotype) are normalized to the mean calculated for the WT. Different letters indicate significant differences between lines ($P < 0.05$).

PGDH1 mutants (*c-pgdh1-2*) and in double *PGDH1/PGDH3* mutants (c-*pgdh1-2 pgdh3-1*). Unlike *PGDH2*, the expression of *PGDH3* was not induced but repressed in both *c-pgdh1-2* and *c-pgdh1-2 pgdh2-3* backgrounds. These results indicated that the absence of *PGDH1* triggers the induction of *PGDH2*, while the absence of *PGDH1* or even both *PGDH1* and *PGDH2* has the opposite effect on *PGDH3* expression, pointing to a negative interaction between *PGDH3* and the other two *PGDH* genes at transcriptional level. In roots, no changes in *PGDH2* gene expression were found in mutants *c-pgdh1-2* and *c-pgdh1-2 pgdh3-1* (Fig. 10D). *PGDH3* is poorly expressed in roots, but a clear trend to a repression in *c-pgdh1-2* and *c-pgdh1-2 pgdh2-3* was observed, which would support an antagonism between *PGDH3* and the two other genes at transcriptional level.

3.4. PGDH3 activity affects photosynthesis, stomatal conductance and transpiration

We have shown that *PGDH3* mutation attenuates the metabolic and phenotypic changes displayed by the two other *PGDH* mutants. This led us to postulate a function for *PGDH3*, different from that of other *PGDH* genes. In order to further understand the function of *PGDH3*, we performed a co-expression analysis study in all three *PGDH* genes (https:// https://genevestigator.com/). In the case of *PGDH3,* all of the 25 most correlated genes coded for chloroplast located proteins (Table 1), which agreed with the specific expression pattern of this gene in photosynthetic organs. Most of these genes were involved in photosynthetic processes, mainly with light related reactions. Accordingly, eight

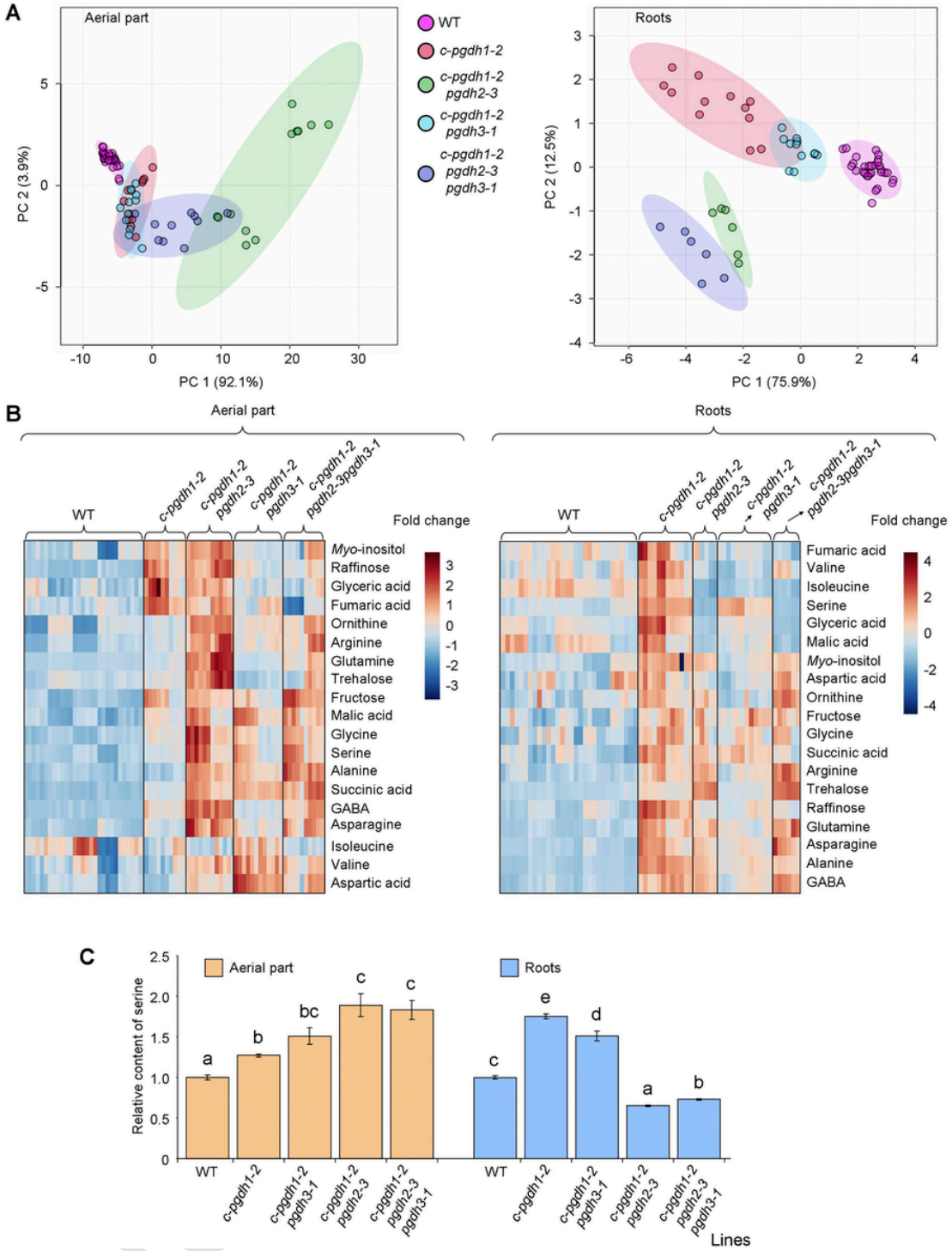

Fig. 8. Metabolite profile of *PGDH* family double and triple mutants (*c-pgdh1-2 pgdh2-3, c-pgdh1-2 pgdh3-1, c-pgdh1-2 pgdh2-3 pgdh3-1*). (A) Principal component analysis (PCA) of the metabolite profiles of *PGDH* mutant lines in aerial parts (AP) and roots. Data from the GC–MS analysis were evaluated using the PCA with the two first components accounting for at least 88 % of total metabolic variance. Values in parenthesis gives the relative contribution of each component to the total variance observed in the dataset. (B) Most relevant changes in the metabolite content of AP and roots of *PGDH* mutants as compared with the wild type (WT). Values of the relative metabolic contents are presented as a heat map. (C) Relative Ser content in different lines. Values represent the mean ± SE, $n \geq 6$ pools of 40 plants from two different lines for each genotype. Different letters indicate significant differences between lines ($P < 0.05$). Detailed results of the assay are presented in Supplementary Tables S4 and S5.

of them code for subunits of the NAD(P)H dehydrogenase like (NDH) complex present in the thylakoid membrane of chloroplasts (NDHM, NDHN, PNSB1, NDHU, PNSB3, PNSL3, PNSL1, CRR3). Also, members of the PGR5 complex (PGRL1A), the ATP synthase complex (ATPD), or proteins involved in the assembly of PSII/PSI complexes (LHCA6, TIC62, ZKT/MET1, MPH1) were found. Finally, some of the co-expressed genes coded for proteins involved in the carbon fixing reactions of photosynthesis (SBPASE, GAPB, RBCSB-1B). The photosynthesis related co-expression pattern was not observed with *PGDH1* and *PGDH2* (Supplementary Tables S6 and S7). Accordingly, we measured the effect of *PGDH3* deficiency in photosynthesis and other photosynthetic related parameters. Both *pgdh3-1* and *pgdh3-2* showed reduced

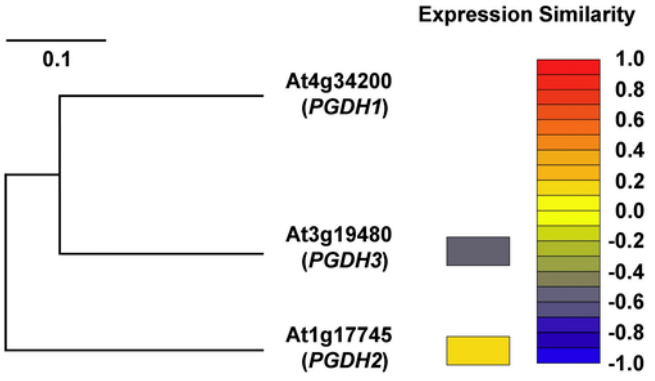

Fig. 9. Phylogenetic and expression analysis of the Arabidopsis *PGDH* genes. The phylogenetic tree was constructed with nucleotide sequences of *PGDH* genes, as described in Materials and Methods. On the right hand, the gene expression analysis using the expressolog tree viewer tool (http://bar.utoronto.ca/), is indicated by a heat map.

net carbon assimilation and quantum efficiency of PSII (Table 2). A lower stomata conductance and transpiration rate was also observed in the mutants. Interestingly, the photorespiratory activity, that could account for the higher Ser levels in these mutants was not higher compared to WT.

4. Discussion

4.1. PGDH2 and PGDH3 contribute to plant development

We have shown that the growth phenotype of the *c-pgdh1* mutants is weaker than that of the *c-psp1-1* mutants in all lines studied, which makes statistically unlikely that the differences observed were due to residual different gene expression or enzyme activity in the two conditional mutants. Thus, these phenotypic differences between *c-pgdh1* and *c-psp1-1* mutants suggests that *PGDH2* and *PGDH3* could play a role in plant development. In a WT background, *PGDH3* deficient lines displayed growth phenotypes when grown either *in vitro* or in greenhouse conditions while *PGDH2* mutants only showed a reduced growth in greenhouse conditions. These results could suggest either that *PGDH3* deficiency affects plant growth more than *PGDH2* deficiency, or that *PGDH1* activity can compensate *PGDH2*'s function in growth better than that of *PGDH3*. Supporting the latter idea are the phenotypes observed in the *c-pgdh1* mutant background, where *PGDH2* deficiency led to stronger growth phenotypes than *PGDH3* deficiency in all conditions assayed. Accordingly, we conclude that *PGDH1* activity can compensate growth phenotypes associated with *PGDH2* better than those associated with *PGDH3* deficiency. We can also conclude that *PGDH1* is

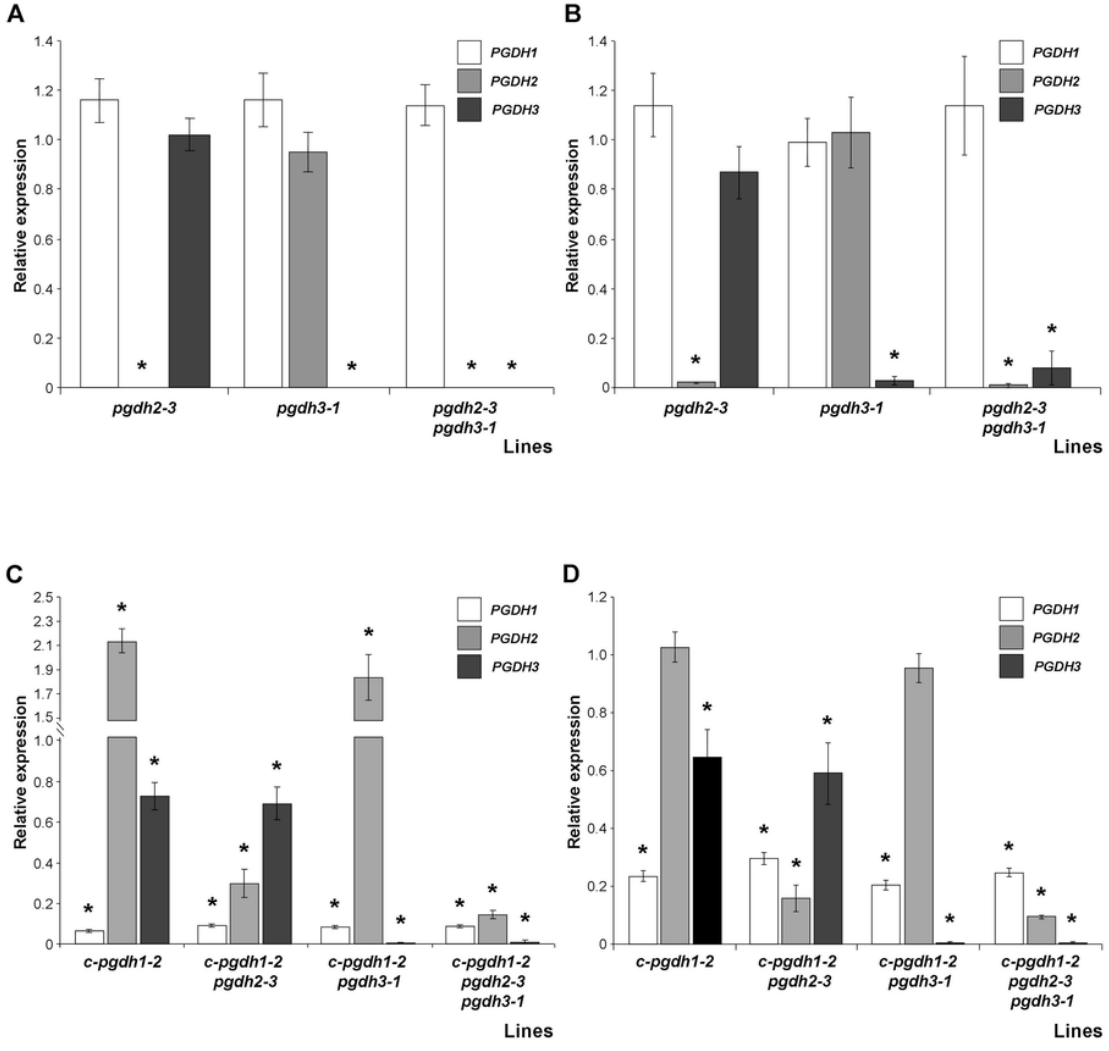

Fig. 10. *PGDH* gene family expression analysis in 15-day-old mutant seedlings grown in plates as compared to wild type (WT). (A, B) qRT-PCR expression analysis in *pgdh2-3, pgdh3-1* and *pgdh2-3 pgdh3-1* aerial parts (AP), (A), and roots (B). (C, D) qRT-PCR expression analysis in *c-pgdh1-2, c-pgdh1-2 pgdh2-3, c-pgdh1-2 pgdh3-1* and *c-pgdh1-2 pgdh2-3 pgdh3-1* aerial parts (AP), (C), and roots (D). Values represent the mean ± SE, n > 4 pools of 30 plants from two different lines for each genotype. * Significantly different to WT ($P < 0.05$).

Table 1
Genes co-expressed with *PGDH3* according to the Genevestigator tool (https://genevestigator.com/). Dataset: 799 perturbations from data selection: At_RNAseq_ARABI_GL-6.

AGI Number	Gene Name	Pearson Score	Description
AT1G19150	*LHCA6*	0.91	PSI type II chlorophyll a/b-binding protein (Lhca2*1) mRNA. Forms the form the NDH-PSI supercomplex
AT4G37925	*NDHM*	0.90	Subunit NDH-M of NAD(P)H:plastoquinone dehydrogenase complex (Ndh complex) present in the thylakoid membrane of chloroplasts.
AT5G58260	*ndhN*	0.90	Encodes subunit NDH-N of NAD(P)H:plastoquinone dehydrogenase complex (Ndh complex) present in the thylakoid membrane of chloroplasts.
AT1G15980	*PNSB1*	0.89	encodes a novel subunit of the chloroplast NAD(P)H dehydrogenase complex, involved in cyclic electron flow around photosystem I to produce ATP.
AT5G21430	*ndhU*	0.89	Chlororespiratory reduction L, CRRL, NADH dehydrogenase-like complex U, NDHU
AT1G09340	*CSP41B*	0.88	Encodes CHLOROPLAST RNA BINDING (CRB), a putative RNA-binding protein. CRB is important for the proper functioning of the chloroplast.
AT3G10060	*FKBP16-4*	0.88	Chloroplastic peptidyl-prolyl cis-trans isomerase activity
AT5G23060	*CAS*	0.87	Chloroplast-localized protein that modulates cytoplasmic Ca2 + concentration and is crucial for proper stomatal regulation in response to elevations of external Ca2 + .
AT2G01590	*CRR3*	0.87	Likely a subunit of the chloroplast NAD(P)H dehydrogenase complex, involved in PSI cyclic electron transport.
AT3G18890	*TIC62*	0.87	TRANSLOCON AT THE INNER ENVELOPE MEMBRANE OF CHLOROPLASTS 62
AT1G55480	*ZKT*	0.87	MET1 Is a Thylakoid-Associated TPR Protein Involved in Photosystem II Supercomplex Formation and Repair in Arabidopsis
AT3G16250	*PNSB3*	0.87	Subunit of the chloroplast NAD(P)H dehydrogenase complex, involved in cyclic electron flow around photosystem I to produce ATP. Contains a 4Fe-4S cluster.
AT3G55800	*SBPASE*	0.86	Chloroplastic enzyme sedoheptulose-1,7-bisphosphatase (SBPase), involved in the carbon reduction of the Calvin cycle. I
AT5G07020	*MPH1*	0.86	Integral thylakoid membrane protein that interacts with PSII core complexes and contributes to the maintenance of PSII homeostasis upon exposure to photoinhibitory light conditions by participating in the protection and stabilization of PSII under photoinhibitory stress.
AT1G49380	*CCS1*	0.86	cytochrome c biogenesis protein family, CHLOROPLASTIC,
AT3G63140	*CSP41A*	0.86	Protein with ribonuclease activity that is involved in plastid rRNA maturation.
AT3G01440	*PNSL3*	0.85	Subunit of the NAD(P)H complex located in the chloroplast thylakoid lumen.
AT4G09650	*ATPD*	0.85	Chloroplast ATPase delta-subunit. The mRNA is cell-to-cell mobile.
AT4G22890	*PGRL1A*	0.85	PGRL1A, a transmembrane protein present in thylakoids.. Plants lacking PGRL1 show perturbation of cyclic electron flow, similar to PGR5-deficient plants. PGRL1 and PGR5 interact physically and associate with PSI (photosystem I).
AT1G42970	*GAPB*	0.85	Chloroplast localized glyceraldehyde-3-phosphate dehydrogenase that can use both NADH and NADPH to reduce 1,3-diphosphate glycerate.
AT5G38430	*RBCS-1B*	0.85	Member of the Rubisco small subunit (RBCS) multigene family.
AT1G18060	*FBN-LIKE*	0.85	localized to chloroplasts
–	*PAP12*	0.85	localized to chloroplasts plastid lipid associated protein
AT4G28660	*PSB28*	0.85	Similar to PsbW subunit of photosystem II.
AT2G39470	*PNSL1*	0.85	PsbP-like protein 2;(source:Araport11)

the major contributor of the family to plant vegetative growth, as already stated for embryo and male gametophyte development [7,11].

4.2. PGDH1 and PGDH2 are more functionally related to each other than with PGDH3

The phylogenetic analysis revealed that *PGDH1* and *PGDH3* are the most closely related genes. However, their expression pattern is markedly different, not only at organ/tissue/cellular level [7,11] but also under different environmental conditions. In Arabidopsis, *PGDH1* and *PGDH2* have a more similar expression pattern to each other than to *PGDH3*. Both *PGDH1* and *PGDH2* are highly expressed in heterotrophic tissue, especially in the vasculature, while *PGDH3* is almost exclusively expressed in autotrophic tissues. The more drastic growth phenotypes of *PGDH1* mutants could be related to its function in specific cell types such as meristems [7,11].

The metabolite profile of *pgdh2-3* and *pgdh3-1* was clearly different to that of the WT, which indicates that both genes are metabolically functional in the plant. Besides, the mutant metabolic profiles were also different from one another. The metabolic changes in *pgdh3-1* were more pronounced in the AP than in roots, while in the opposite trend was found in *pgdh2-3*. For instance, in the *pgdh3-1* AP, 68 % of the identified metabolites changed by more than 25 % compared to the WT, while only 20 % of them were modified by more than 25 % in roots. Opposite, in the *pgdh2-3* AP, only 40 % of the metabolites changed more than 25 % while in roots this percentage increased to 64 %. These results would indicate that PGDH3 function is more important in the AP while that of PGDH2 is more important in roots as already suggested by the gene expression analysis. They also indicate that PGDH2 and PGDH3 may be involved in different processes. Interestingly, the PCA of the metabolite profile of the *pgdh2-3 pgdh3-1* double mutant showed a partial overlap with that of the WT, suggesting that the double mutation lead to a partial metabolic compensation.

Comparison of the metabolite profile of double mutants including *PGDH1* combined with *PGDH2* or *PGDH3* (*c-pgdh1-2 pgdh2-3, c-pgdh1-2 pgdh3-1*) and the triple *PGDH* mutant (*c-pgdh1-2 pgdh2-3 pgdh3-1*) showed a generalized increase in the metabolite level compared to controls, especially of amino acids. This generalized increase could be realated to PGDH functions but also with the drastic growth reduction observed in these mutants. Interestingly, the absence of both *PGDH1* and *PGDH2* produced more drastic differences in the of the AP than those found in the triple mutant, supporting a compensatory role of *PGDH3* with the other two genes of the family.

Gene expression analysis showed that when *PGDH1* is fully active, there are no changes in the *PGDH2* or *PGDH3* expression in the single *pgdh3-1 or pgdh2-3* mutants, respectively. However, a reduced *PGDH1* expression (*c-pghd1-2* background) affected the expression of the two other genes differently, supporting its role as main gene of the family. Accordingly, *PGDH3* expression was repressed in both *PGDH1* single and *PGDH1/PGDH2* double mutant backgrounds, which supported an opposite expression pattern of *PGDH3* with the other two genes of the family. Previous studies also sustain an opposite expression pattern of

Table 2
Photosynthetic parameters in *PGDH3* mutants. Photosynthetic rate (AN; μmol m^{-2} s^{-1}), stomatal conductance (gs; mol m^{-2} s^{-1}), substomatal CO_2 concentration (Ci; mol/mol air), transpiration rate (E; mmol m^{-2} s^{-1}) effective photochemical yield of Photosystem II (PhiPS2) and photorespiration rate (PR; μmol m^{-2} s^{-1}) are shown. Each value is the mean (± SE) of 10 independent determinations. For each parameter, different letters indicate significant differences between groups ($P < 0.05$). NS: not significant.

Genotype	A_N	g_s	C_i	E	PhiPS2	PR
WT	7.14 ± 0.10 a	0.145 ± 0.004 a	313 ± 2	2.62 ± 0.06 a	0.117 ± 0.001 a	1.15 ± 0.02 a
pgdh3-1	5.20 ± 0.17b	0.102 ± 0.005 b	312 ± 3	1.85 ± 0.07 b	0.098 ± 0.003 b	1.05 ± 0.05 ab
pgdh3-2	4.94 ± 0.16 b	0.105 ± 0.005 b	319 ± 4	1.89 ± 0.08 b	0.087 ± 0.002 b	0.78 ± 0.05 b

PGDH1/PGDH2 and *PGDH3*. For instance, we reported that *PGDH1/PGDH2* are induced by abiotic stresses such as salinity while *PGDH3* is repressed [26]. In this respect, we also reported that *PGDH3* expression is repressed in lines overexpressing *PGDH1*, especially under salt stress conditions [26]. However, *PGDH1* and *PGDH2* are only repressed in plants overexpressing *PGDH3* under control conditions, but not under salt stress conditions. The biochemical behavior of PGDH2 and PGDH3 isoforms is also different, with PGDH3 being highly sensitive to Ser feed-back inhibition while PGDH2 activity is completely insensitive to this amino acid [7,27].

The growth phenotypes of double and triple mutants indicated that the *c-pgdh1-2 pgdh2-3* double mutant displayed the most dramatic growth reductions, even more dramatic than those of the triple mutant. Furthermore, they showed that the activity of PGDH3 in the AP, where it is mostly expressed, is somehow detrimental in a double mutant *c-pgdh1-2 pgdh2-3* background, but not in the single mutant *c-pgdh1-2*, demonstrating that the *PGDH3* was more specifically compensating *PGDH2* function in growth as already suggested in the double mutant *pgdh2-3 pgdh3-1* background.

Our results indicate that *PGDH1* and *PGDH2* are partially redundant, at least in the AP, where *PGDH2* is induced in *c-pgdh1-2* mutant backgrounds. *In silico* gene expression analysis showed a positive correlation between *PGDH1* and *PGDH2*. This positive correlation is not only restricted to the transcriptional level. According to the Arabidopsis interactome map, a physical interaction between *PGDH1* and *PGDH2* has been described (Supplementary Fig. S5; [28]). The lack of growth phenotype of the *pgdh2-3* single mutant along with the much stronger phenotypes of c-*pgdh1-2 pgdh2-3* double mutant as compared to single c-*pgdh1-2* mutant, led us to postulate that PGDH1 and PGDH2 activities are probably required to provide Ser to similar processes. *PGDH2* could cooperate/suport *PGDH1* functions in specific conditions. For instance, *PGDH2* is highly induced in biotic or abiotic stresses ((https://genevestigator.com/) where additional supply of Ser could be required.

On the other hand, *c-pgdh1-2 pgdh3-1* double mutants have also stronger growth phenotypes than *c-pgdh1-2* single mutants, which could suggest that *PGDH1* and *PGDH3* are also partially redundant. However, we have to keep in mind that both single *c-pgdh1-2* and *pgdh3-1* mutants already show growth phenotypes and thus the stronger phenotype of the double mutant does not necessarily indicate a redundancy but an additive effect of each single mutant phenotype. The fact that *PGDH3* is repressed in a c-*pgdh1-2* mutant background rather than induced would support this later idea.

We found that there is a negative correlation between growth inhibition and Ser-steady-state levels in the AP. Thus, the highest levels of Ser in the AP were found in the *c-pgdh1-2 pgdh2-3* double mutant and in the *c-pgdh1-2 pgdh2-3 pgdh3-1* triple mutant. The high steady state Ser levels in the AP of these mutant lines could be due to a general increase in the amino acid content associated to the dramatically reduced growth. However, it could also be due to the increased activity of the glycerate pathway in the AP and the subsequent Ser transport to the roots. We have previously hypothesized that there is an interaction between the PPSB and the glycolate pathway to maintain plant Ser homeostasis [8]. This would imply induction of Ser biosynthesis in photosynthetic organs and transport to heterotrophic organs such as roots.

Unlike in the AP, the lines which exhibited the strongest growth reductions showed the lowest Ser levels in roots. *PGDH2* seem to play a crucial role in the supply of Ser through the PPSB that, as a whole, could be quantitatively even more important than *PGDH1*. In both genetic backgrounds (WT or *c-pgdh1-2*) *PGDH2* mutations reduced Ser pools in roots, even despite drastic root growth reduction. However, no Ser reduction is seen in *PGDH1* mutants in the WT background (*c-pgdh1-2*), probably due to the induction of *PGDH2*. The fact that PGDH2 is the PGDH isoform whose activity is more insensitive to Ser feed-back inhibition would also support our hypothesis. Regarding *PGDH3*, the lack of this isoform in the AP, where it is mostly active, never resulted in a reduction of the levels of Ser pools neither in a WT, nor in a *c-pgdh1-2* mutant or a *c-pgdh1-2 pgdh2-3* mutant background. All these results reinforce the hypothesis that *PGDH1* and *PGDH2* cooperated in the PPSB to supply Ser to specific plant organs, and that *PGDH3* may have additional functions in specific cell types which may or may not be directly related to Ser supply itself. In this respect, *PGDH1* and *PGDH2* transcriptionally interact with other PPSB genes such as *PSAT1*, *PSAT2*, but all them are in a different transcriptional network to that of *PGDH3* (Supplementary Fig. S5). Besides, the fact that PGDH3 is the PGDH isoform whose activity is most highly sensitive to Ser feed-back inhibition would also agree with our hypothesis. Accordingly, the growth phenotype defects of *c-psp1-1* mutants, in which the PPSB is completely blocked, is similar to that of *PGDH1/PGDH2* double mutants (*c-pgdh1-2 pgdh2-3)*, which again would strongly indicate that PGDH1 and PGDH2 are the main enzymes providing substrates for PSP1 through the PPSB.

4.3. Physiological function of PGDH3

In the co-expression experiments we found that most of the highly *PGDH3* co-expressed genes were related to photosynthesis, especially with the light dependent reactions. This pattern was not observed in *PGDH1* or *PGDH2*. In angiosperms, there are two pathways involved in the PSI cyclic electron transport, the antimycin A resistant pathway dependent on PGR5 (Proton Gradient Regulation 5) and PGRL1 complex (PGR5-Like Photosythesis Phenotype 1), [29–32], and the NDH-dependent pathway [31,33]. Mutants of the antimycin A resistant pathway, such as *pgr5* have reduced ability to dissipate excessively light energy from PSII, being concluded that the complex containing PGR5/PGRL1 is involved in the switch between linear and cyclic electron transport [29–31]. *PGRL1A* is co-expressed with *PGDH3*, suggesting that it could somehow interacts with PSII activity. Other genes related to PSII were also co-expressed with *PGDH3*, such as *ZKT/MET* or *MPH1*. MET1 is a thylakoid-associated protein involved in PSII supercomplex formation and repair in Arabidopsis [34]. MPH1 has been suggested to play a role in the protection and stabilization of PSII under high-light intensity [35]. In accordance with the analysis of co-expression, we found that *PGDH3* mutants have reduced quantum efficiency of PSII.

We also found that many components of the NDH-dependent pathway (*NDHM, NDHN, PNSB1, NDHU, PNSB3, PNSL3, PNSL1, CRR3, LHCA6*) were co-expressed with *PGDH3*. The chloroplast NDH complex is associated to PSI forming the NDH-PSI supercomplex [31]. This NDH complex reduces the plastoquinone pool in the cyclic electron flow

around PSI, supplying, along with the antimycin A resistant pathway, extra-ATP and compensating for the ATP/NADPH production, particularly under environmental stress conditions [31]. PGDH activity is coupled to NADH production. We therefore speculate that PGDH3 activity is tightly associated/interacting with the photosynthetic electron flux, probably *via* NADH production and that *PGDH3* mutation perturbs the equilibrium between ATP/NAD(P)H required for plastid metabolism, thus impairing photosynthetic electron flux.

In addition to PSII quantum efficiency, other photosynthetic parameters such as net CO_2 assimilation, and stomata opening were affected in *PGDH3* mutants. These alterations could be the consequence of reduced PSII quantum efficiency in *PGDH3* mutants, but a direct interaction of PGHD3 activity with these photosynthetic processes may not be discarded. In this respect, we found some *PGDH3* co-expressed genes which participate in the carbon fixing reactions of photosynthesis (*SBPASE, GAPB, RBCSB-1B*) or in the stomata regulation such as CAS, a chloroplast protein crucial for proper stomatal regulation in response to elevations of external Ca^{2+}.

The metabolomic study performed here is biased in that no photosynthetic metabolites were detected, since most of them are phosphorylated and cannot be accurately determined by the gas chromatography-mass spectrometry method. Nonetheless, one of the most important metabolite changes distinguishing *PGDH3* mutants from others is glyceric acid. This metabolite was reduced in *pgdh3-1* more than in *pgdh2-3*, while in the double c-*pgdh1-2 pgdh3-1* and triple c-*pgdh1-2 pgdh2-3 pgdh3-1* background, the glyceric acid levels were always reduced as compared to the single c-*pgdh1-2* and double c-*pgdh1-2 pgdh2-3*, respectively. Glyceric acid could be synthesized from 3-phosphoglycerate, the substrate of PGDHs, in a reaction catalyze by phosphoglycerate phosphatase. The 3-phosphoglycerate is also the first product of Calvin-Benson-Bassam cycle. Since we demonstrated that *pgdh3-1* mutants show reduced photosynthetic rate, the 3-phosphoglycerate content could be diminished in this mutant which, in turn, would impact on the glyceric acid levels measured in this study.

Our results suggest that PGDH gene family underwent functional evolutive divergence probably associated to their cell-type specific localization. This hypothesis would be supported by fact that *PGDH3* is expressed in fully active photosynthetic cells in mature leaves where it co-exist with the glycolate pathway. This environment could lead to a new function for *PGDH3* not related with Ser biosynthesis. Accordingly, *PGDH3* is the only PGDH isoform which accumulates under fluctuating light conditions [36,37].

Another important question that remains to be clarified is why the *PGDH3* mutations improve growth of the other *PGDH* mutants. As this improving growth effect was not observed in a WT background, the most plausible explanation is that the reduced photosynthetic activity may be beneficial for *PGDH* mutants. Arabidopsis lines with reduced PPSB activity accumulated amino acids and sugars which can not be used for growth [9]. Most likely, a reduced photosynthetic activity may modulate/balance the carbohydrate and amino acid homeostasis which may benefit growth recovery.

5. Conclusions

From this work we can corroborate that *PGDH1* is the most important gene of the PGDH family, probably associated to its broader expression pattern, especially in specific cell types such as root meristems. *PGDH2* contribution to plant vegetative growth is greater than that of *PGDH3*. *PGDH1* and *PGDH2* would perform similar functions related to Ser metabolism through PPSB. *PGDH3* loss, however, partially compensate mutations in *PGDH2*, and could play an additional role associated to photosynthesis, although future work will be required to confirm this later hypothesis.

Author's contributions

R.C-A., J.M-B., S.R-T., A.D.A., and S.G-N participated in investigation, methodology, formal analysis and provided resources. A.T-M. participated in software. A.R.F. participated in supervision and validation. R.C-A., J.M-B. S.R-T., A.D.A., S.G-N and A.R.F. participated in writing –review and editing. S.R-T and R.C-A participated in data curation. R.R. participated in writing the original draft, conceptualization, supervision and funding acquisition.

Data availability statement

All data supporting the findings of this study are available within the paper and within its supplementary materials published online. The material supporting the findings of this study are available from the corresponding author, (Author name), upon request.

Declaration of Competing Interest

The authors report no declarations of interest.

Acknowledgements

We thank SCIE of the Universitat de València for technical assistance. We thank Saleh Alseekh for assistance in the analysis of GC–MS samples. This research was supported by the Spanish Government and the European Union (FEDER/BFU2015-64204R, PID2019-107174GB-I00 to R.R. and BES-2016-077943 to R. C-A.), the Valencian Regional Government to S.R-T. (APOSTD/2017/132).

Appendix A. Supplementary data

Supplementary material related to this article can be found, in the online version, at doi:https://doi.org/10.1016/j.plantsci.2021.110863.

References

[1] R. Ros, J. Muñoz-Bertomeu, S. Krueger, Serine in plants: biosynthesis, metabolism, and functions, Trends Plant Sci. 19 (2014) 564–569.
[2] H. Bauwe, M. Hagemann, A.R. Fernie, Photorespiration: players, partners and origin, Trends Plant Sci. 15 (2010) 330–336.
[3] A.U. Igamberdiev, L.A. Kleczkowski, The glycerate and phosphorylated pathways of serine synthesis in plants: The branches of plant glycolysis linking carbon and nitrogen metabolism, Front. Plant Sci. 9 (2018) 318.
[4] N.E. Tolbert, The C_2 oxidative photosynthetic carbon cycle, Annu. Rev. Plant Physiol. Plant Mol. Biol. 48 (1997) 1–25.
[5] R. Douce, J. Bourguignon, M. Neuburger, F. Rebeille, The glycine decarboxylase system: a fascinating complex, Trends Plant Sci. 6 (2001) 167–176.
[6] S.P. Robinson, 3-Phosphoglycerate phosphatase activity in chloroplast preparations as a result of contamination by acid phosphatase, Plant Physiol. 70 (1982) 645–648.
[7] R.M. Benstein, K. Ludewig, S. Wulfert, S. Wittek, T. Gigolashvili, H. Frerigmann, M. Gierth, U.I. Flügge, S. Krueger, Arabidopsis phosphoglycerate dehydrogenase1 of the phosphoserine pathway is essential for development and required for ammonium assimilation and tryptophan biosynthesis, Plant Cell25 (2013) 5011–5029.
[8] A.D. Anoman, M. Flores-Tornero, R.M. Benstein, S. Blau, S. Rosa-Téllez, A. Bräutigam, A.R. Fernie, J. Muñoz-Bertomeu, S. Schilasky, A.J. Meyer, S. Kopriva, J. Segura, S. Krueger, R. Ros, Deficiency in the phosphorylated pathway of serine biosynthesis perturbs sulfur assimilation, Plant Physiol. 180 (2019) 153–170.
[9] B. Cascales-Miñana, J. Muñoz-Bertomeu, M. Flores-Tornero, A.D. Anoman, J. Pertusa, M. Alaiz, S. Osorio, A.R. Fernie, J. Segura, R. Ros, The phosphorylated pathway of serine biosynthesis is essential both for male gametophyte and embryo development and for root growth in Arabidopsis, Plant Cell25 (2013) 2084–2101.
[10] J. Muñoz-Bertomeu, A. Anoman, M. Flores-Tornero, W. Toujani, S. Rosa-Tellez, A.R. Fernie, S. Roje, J. Segura, R. Ros, The essential role of the phosphorylated pathway of serine biosynthesis in Arabidopsis, Plant Signal. Behav. 8 (2013), e27104.
[11] W. Toujani, J. Muñoz-Bertomeu, M. Flores-Tornero, S. Rosa-Téllez, A.D. Anoman, S. Alseekh, A.R. Fernie, R. Ros, Functional characterization of the plastidial 3-phosphoglycerate dehydrogenase family in Arabidopsis, Plant Physiol. 163 (2013) 1164–1178.
[12] W. Toujani, J. Muñoz-Bertomeu, M. Flores-Tornero, S. Rosa-Téllez, A. Anoman, R. Ros, Identification of the phosphoglycerate dehydrogenase isoform EDA9 as the es-

sential gene for embryo and male gametophyte development in Arabidopsis, Plant Signal. Behav. 8 (2013), e27207.
[13] S. Wulfert, S. Krueger, Phosphoserine aminotransferase1 is part of the phosphorylated pathways for serine biosynthesis and essential for light and sugar-dependent growth promotion, Front. Plant Sci. 9 (2018) 1712.
[14] R.L. Scholl, S.T. May, D.H. Ware, Seed and molecular resources for Arabidopsis, Plant Physiol. 124 (2000) 1477–1480.
[15] M.D. Curtis, U. Grossniklaus, A gateway cloning vector set for high-throughput functional analysis of genes in planta, Plant Physiol. 133 (2003) 462–469.
[16] S.J. Clough, A.F. Bent, Floral dip: a simplified method for Agrobacterium-mediated transformation of Arabidopsis thaliana, Plant J. 16 (1998) 735–743.
[17] T. Czechowski, M. Stitt, T. Altmann, M.K. Udvardi, W.R. Scheible, Genome-wide identification and testing of superior reference genes for transcript normalization in Arabidopsis, Plant Physiol. 139 (2005) 5–17.
[18] M.W. Pfaffl, A new mathematical model for relative quantification in real-time RT-PCR, Nucleic Acids Res. 29 (2001) e45.
[19] J. Lisec, N. Schauer, J. Kopka, L. Willmitzer, A.R. Fernie, Gas chromatography mass spectrometry-based metabolite profiling in plants, Nat. Protoc. 1 (2006) 387–396.
[20] I. Faus, A. Zabalza, J. Santiago, S.G. Nebauer, M. Royuela, R. Serrano, J. Gadea, Protein kinase GCN2 mediates responses to glyphosate in Arabidopsis, BMC Plant Biol. 15 (2015) 14.
[21] R. Valentini, D. Epron, P. de Angelis, G. Matteucci, E. Dreyer, In situ estimation of net CO_2 assimilation, photosynthetic electron flow and photorespiration in Turkey oak (Q. cerris L.) leaves: diurnal cycles under different levels of water supply, Plant Cell Environ. 18 (1995) 631–640.
[22] S. Kumar, G. Stecher, M. Li, C. Knyaz, K. Tamura, MEGA X: molecular evolutionary genetics analysis across computing platforms, Mol. Biol. Evol. 35 (2018) 1547–1549.
[23] R.V. Patel, H.K. Nahal, R. Breit, N.J. Provart, BAR expressolog identification: Expression profile similarity ranking of homologous genes in plant species, Plant J. 71 (2012) 1038–1050.
[24] T. Hruz, O. Laule, G. Szabo, F. Wessendorp, S. Bleuler, L. Oertle, P. Widmayer, W. Gruissem, P. Zimmermann, Genevestigator V3: a reference expression database for the meta-analysis of transcriptomes, Adv. Bioinf. (2008), 420747.
[25] D. Warde-Farley, S.L. Donaldson, O. Comes, K. Zuberi, R. Badrawi, P. Chao, M. Franz, C. Grouios, F. Kazi, C.T. Lopes, A. Maitland, S. Mostafavi, J. Montojo, Q. Shao, G. Wright, G.D. Bader, Q. Morris, The GeneMANIA prediction server: Biological network integration for gene prioritization and predicting gene function, Nucleic Acids Res. 38 (2010) W214–W220.
[26] S. Rosa-Téllez, A.D. Anoman, A. Alcántara-Enguídanos, R.A. Garza-Aguirre, S. Alseekh, R. Ros, PGDH family genes differentially affect Arabidopsis tolerance to salt stress, Plant Sci. 290 (2020), 110284.
[27] E. Okamura, M.Y. Hirai, Novel regulatory mechanism of serine biosynthesis associated with 3-phosphoglycerate dehydrogenase in Arabidopsis thaliana, Sci. Rep. 7 (2017) 3533.
[28] AIMP, Evidence for network evolution in an arabidopsis interactome map by the arabidopsis interactome mapping consortium, Science333 (2011) 601–607.
[29] Y. Munekage, M. Hojo, J. Meurer, T. Endo, M. Tasaka, T. Shikanai, PGR5 is involved in cyclic electron flow around photosystem I and is essential for photoprotection in Arabidopsis, Cell110 (2002) 361–371.
[30] G. DalCorso, P. Pesaresi, S. Masiero, E. Aseeva, D. Schünemann, G. Finazzi, P. Joliot, R. Barbato, D. Leister, A complex containing PGRL1 and PGR5 is involved in the switch between linear and cyclic electron flow in Arabidopsis, Cell132 (2008) 273–285.
[31] T. Shikanai, Chloroplast NDH: a different enzyme with a structure similar to that of respiratory NADH dehydrogenase, Biochim. Biophys. Acta Bioenerg. 1857 (2016) 1015–1022.
[32] K. Sugimoto, Y. Okegawa, A. Tohri, T.A. Long, S.F. Covert, T. Hisabori, T. Shikanai, A single amino acid alteration in PGR5 confers resistance to antimycin a in cyclic electron transport around PSI, Plant Cell Physiol. 54 (2013) 1525–1534.
[33] K. Ifuku, T. Endo, T. Shikanai, E.M. Aro, Structure of the chloroplast NADH dehydrogenase-like complex: nomenclature for nuclear-encoded subunits, Plant Cell Physiol. 52 (2011) 1560–1568.
[34] N.H. Bhuiyan, G. Friso, A. Poliakov, L. Ponnala, K.J. Van Wijk, MET1 is a thylakoid-associated TPR protein involved in photosystem II supercomplex formation and repair in Arabidopsis, Plant Cell27 (2015) 262–285.
[35] J. Liu, R.L. Last, A land plant-specific thylakoid membrane protein contributes to photosystem II maintenance in Arabidopsis thaliana, Plant J. 82 (2015) 731–743.
[36] S. Niedermaier, T. Schneider, M.O. Bahl, S. Matsubara, P.F. Huesgen, Photoprotective acclimation of the Arabidopsis thaliana leaf proteome to fluctuating light, Front. Genet. 11 (2020) 154.
[37] T. Schneider, A. Bolger, J. Zeier, S. Preiskowski, V. Benes, S. Trenkamp, B. Usadel, E.M. Farré, S. Matsubara, Fluctuating light interacts with time of day and leaf development stage to reprogram gene expression, Plant Physiol. 179 (2019) 1632–1657.